guide," *J. Inst. Elec. Commun. Eng. Jap.*, vol. 47, Mar. 1964.
[6] Von S. Seldmair, "Ein breitbandiges Dämpfungsglied zur gleichzeitigen Bedämpfung Höherer $H_{0n}$-Wellen in $H_{01}$-Übertragung-sleitungen," *Frequenz*, vol. 22, p. 118, 1968.
[7] S. Shimada, "$TE_{02}$ mode filter for $TE_{01}$ mode circular waveguide at millimeter wavelengths," *Rev. Elec. Commun. Lab.*, vol. 16, Jan.–Feb. 1968.
[8] K. Hashimoto *et al.*, "Wave coupled $TE_{02}$ mode filters," *Rev. Elec. Commun. Lab.*, vol. 22, Jan.–Feb. 1974.
[9] K. Hashimoto *et al.*, "Circular $TE_{0n}$ mode filters for a guided millimeter-wave transmission," in *1973 G-MTT Int. Microwave Symp. Dig.*, pp. 19–21, 1973.
[10] M. V. Persikov, "Brief communication filter for the $H_{02}$-wave in a circular waveguide," *Radio-teknika Electron.*, vol. 6, p. 444, 1961.
[11] J. L. Altman, *Microwave Circuits*. New York: Van Nostrand, 1964.
[12] K. Kondoh *et al.*, "Analysis of transmission characteristics of circular waveguide installed in cable tunnels," *Rev. Elec. Commun. Lab.*, vol. 19, Nov.–Dec. 1971.

# Wide-Band Varactor-Tuned Coaxial Oscillators

COLIN D. CORBEY, ROBERT DAVIES, AND ROBERT A. GOUGH

*Abstract*—**An experimental investigation into the effects of package and circuit reactances on wide-band varactor-tuned oscillators is described. The results are used to design an *X*-band Gunn coaxial oscillator with a tuning range in excess of 3 GHz. It is shown that the stray reactances, junction capacitance, and bond-wire inductance affect the varactor tuning characteristics. The characteristics are conveniently displayed by the reflection phase variation with tuning voltage and frequency. A general theory for wide-band varactor-tuned oscillators is presented which is related to the impedance characteristics. These results are used to design three coaxial varactor-tuned oscillators. The first two oscillators are series arrangements while the third oscillator is a parallel arrangement. A simple circuit technique is used to improve the tuning range of each arrangement. This technique is shown to increase the coupling to the varactor diode and decrease the oscillator *Q* by reactance compensation.**

## I. INTRODUCTION

WHILE considerable microwave-circuit design information exists for varactor-tuned oscillators, little has been done to optimize the wide-band operation. The more successful wide-band oscillators use varactor diodes either in miniature packages [1], [2] or unencapsulated in microwave integrated circuits [3]. In the present investigation, attempts are made to obtain wide-band operation at *X* band using the standard S4 [4] package by appropriate choice of circuit impedance, varactor-diode parameters, including bond-wire inductance, and diode mounting arrangements. Other authors [5] have studied the importance of package parasitics in the design of transferred-electron amplifiers and were able to optimize the package for *X*–*Ku*-band applications.

The design feature of wide-band varactor-tuned oscillators is that the varactor junction capacitance should be the dominant resonating reactance. Although the resonant frequencies of the S4 package are lower than those of the miniature package, large tuning ranges at *X* band have been reported in a coaxial arrangement (1.1 GHz) [6], a full-height waveguide structure (over 1 GHz) [7], and a reduced-height waveguide structure (1.95 GHz) [8]. In this work, coaxial circuits are investigated because of their low *Q* and ease of characterization.

Microwave-diode impedance measurements are shown to substantially agree with calculated values using the equivalent-circuit models developed elsewhere [9]–[11]. A general theory of wide-band varactor-tuned oscillators is presented and the importance of the varactor impedance–voltage relationship as displayed on a Smith chart by the varactor reflection phase variation is discussed. The concept of tuning phase is introduced. The tuning phase is shown to be related to the oscillator tuning range and is dependent on the frequency, circuit stray reactances, bond-wire inductance, and varactor junction capacitance.

Three coaxial varactor-tuned *X*-band Gunn or IMPATT oscillators are finally described; the first two arrangements incorporate the varactor and active devices in series; the third incorporates the devices in parallel. A varactor diode with a large tuning phase is used to realize a varactor tuning range in excess of 3 GHz with a Gunn device.

## II. MICROWAVE-DIODE IMPEDANCE CHARACTERISTICS

Package and circuit parasitic reactances associated with the S4 package in series and shunt-mounted coaxial arrangements have been reported elsewhere [9]–[11], yield-

Manuscript received June 18, 1974; revised May 17, 1975. The work of one of the authors (R.A.G.) was supported by a United Kingdom Science Research Council Grant.

C. D. Corbey and R. Davies are with the Mullard Research Laboratories, Redhill, Surrey, England.

R. A. Gough was with the University of Bradford, Bradford, Yorks., England. He is now with ESTEC, Domeinweg, Noordwijk, The Netherlands.

ing accurate equivalent-circuit models. These models are used in this section to discuss the impedance characteristics of some commercial devices.

### A. Bond-Wire Inductance

A knowledge of bond-wire inductance is necessary since manufacturers use different bond-wire configurations which cause large variations in the inductance [12]. X-ray radiographs of five S4 packages from different manufacturers are given in Fig. 1. Package *A* shows a device which uses a single wire or "nail-bond;" package *B* uses a two wire or "*V*-bond;" package *C* uses a four wire or "*X*-bond;" package *D* uses a multiwire or "mesh" bond; and package *E* shows a device which uses the *V*-bond in a slightly reduced package pillar height. The last radiograph indicates that variations can occur in the internal package geometry.

The bond-wire inductance of the Gunn device was determined from slotted-line impedance measurements at 1 GHz on an unbiased device situated in the end-mounted test fixture. The method is based upon the fact that at 1 GHz the chip parameters are negligible compared with the inductance [13]. Typical values of the Mullard CXY19, which uses a nail-bond, are shown in Table I. The contribution of the Gunn-device reactance to the total reactance is less than 2.5 percent. The results imply that substantial variations can occur for devices employing similar bond-wire configurations.

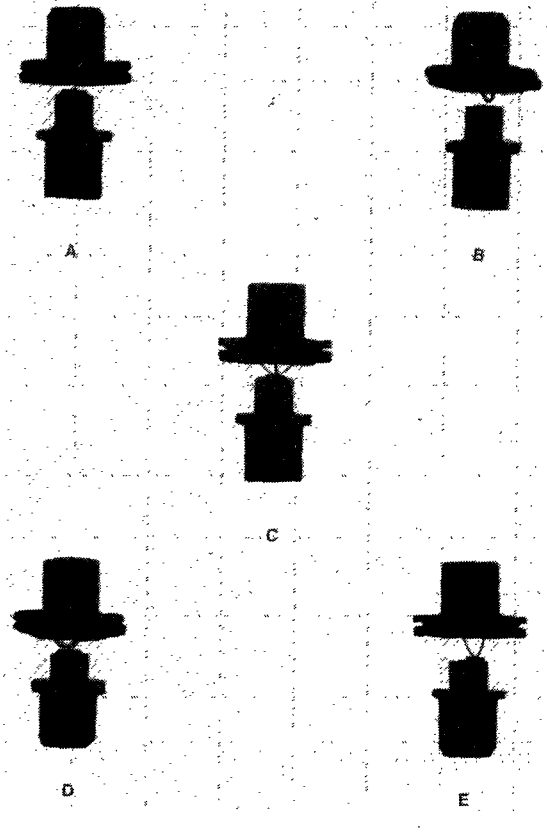


Fig. 1. X-ray radiographs of S4 packaged diodes. *A*—Mullard CXY19. *B*—Gigahertz devices GC-1600. *C*—Microwave Associates ML4707. *D*—Hewlett-Packard 5082-0437. *E*—Microwave Associates ML4707.

TABLE I
BOND-WIRE INDUCTANCE MEASUREMENTS OF FOUR CXY19 DEVICES

| DEVICE NUMBER | TOTAL REACTANCE AT 1 GHz (Ω) | BOND WIRE INDUCTANCE (nH) |
|---|---|---|
| 1 | 6.11 | 0.50 |
| 2 | 7.20 | 0.54 |
| 3 | 7.74 | 0.62 |
| 4 | 6.67 | 0.45 |

TABLE II
BOND-WIRE INDUCTANCE MEASUREMENTS OF THREE VARACTOR-DIODE TYPES

| DIODE TYPE | WIRE INDUCTANCE (nH) |
|---|---|
| BXY53 | 0.38 ± 3% |
| ML4704 | 0.37 ± 4% |
| ML4707 | 0.20 ± 5% |

Bond-wire inductances of IMPATT and varactor diodes were determined from a knowledge of the junction capacitances determined from 1-MHz measurements and the microwave transmission characteristics on the devices [14] situated in the shunt-mounted test fixture shown in [9, fig. 1]. The values of bond-wire inductance were found to be constant to within 10 percent over the bias voltage frequency ranges. The bond-wire inductances of three silicon diodes are given in Table II. The variations of inductance are the maximum deviations over the bias voltage range.

### B. Varactor-Diode Impedance Measurements

Varactor-diode return loss and reflection phase variation over the bias voltage range have been considered since they are invariant under transformation down a uniform lossless transmission line [15]. Measurements were obtained from the use of an automatic network analyzer and a typical set is shown in Fig. 2 at 10 GHz for a series-mounted BXY53 varactor diode over the reverse-bias voltage range 0–50 V. The figure indicates the significance of the embedded condition for the series-mounted test fixture shown in [9, fig. 1]. From Fig. 2 it is seen that the varactor reflection phase variation is improved from 64° for the normal mounting, $l = 0$ mm, to 125° for the embedded mounting, $l = 1.5$ mm.

However, the improved reflection phase variation is accompanied by an increased return loss. Further reflection phase and return-loss measurements are given in Fig. 3 at 9 GHz. Also shown are calculated impedance values obtained from the use of the equivalent-circuit values given in [9, table I], the bond-wire inductances of Table

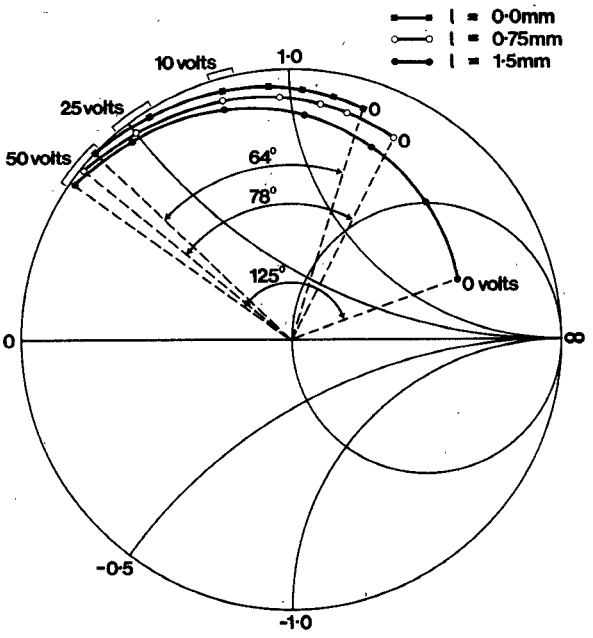


Fig. 2. Varactor-diode impedance of BXY53 at 10 GHz for three embedded depths.

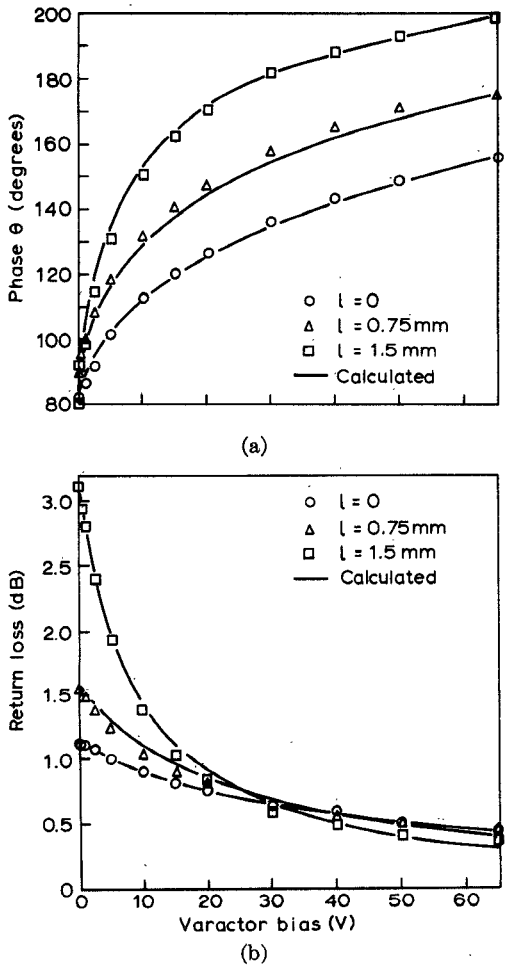


Fig. 3. Varactor-diode impedance of BXY53 at 9 GHz. (a) Phase. (b) Return loss.

II, the low-frequency 1-MHz capacitance-voltage characteristics of Fig. 4(a), and the microwave spreading resistances of Fig. 4(b) which were obtained from transmission-loss measurements [14].

The agreement between measured and calculated values is very good; peak deviations of return loss are less than 0.2 dB and peak deviations of phase are less than 5°. The reflection phase variation for most devices was found to improve upon embedding at $X$ band, and this was accompanied by an increased return loss. However, it was noticed that certain low-capacitance varactors showed the reverse effect.

In order to understand these effects further, the measured and calculated varactor breakdown reflection phase, $\theta_{br}$, and reflection phase variation, $\Delta\theta$, of the BXY53 device are given in Fig. 5(a) and (b) over the frequency range 7–12 GHz. The reflection phase characteristics are as follows.

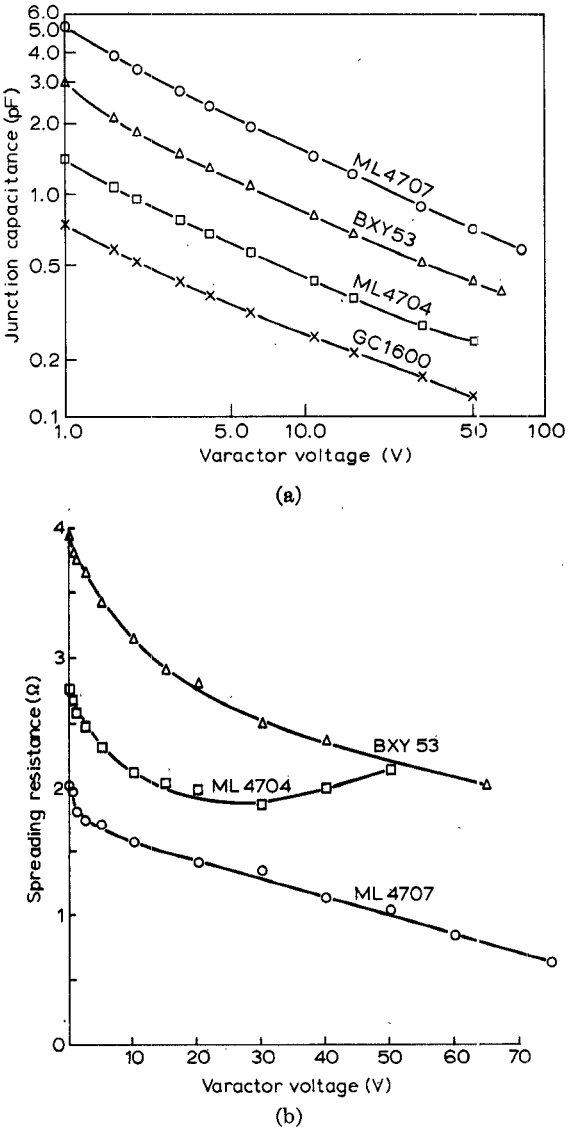


Fig. 4. (a) Low-frequency varactor junction characteristics of ML4707, BXY53, ML4704, and GC1600. (b) Varactor-diode spreading resistance of BXY53, ML4704, and ML4707.

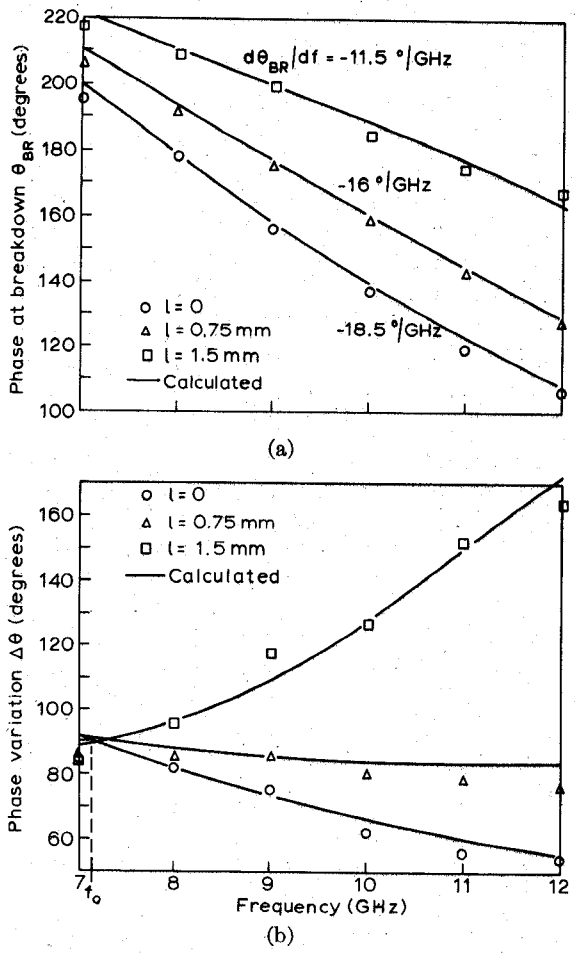


Fig. 5. Varactor-diode impedance-frequency characteristics of BXY53. (a) Breakdown voltage phase. (b) Phase variation from 0 to 50 V.

a) The decrease of $\theta_{br}$ with frequency is almost linear and the slope decreases with increased depths of embedding $l$; e.g., it is seen from Fig. 5(a) that the slope decreases from approximately $-18.5°$/GHz to $-11.5°$/GHz.

b) The series resonant frequency $f_{res}$, at breakdown $\theta_{br} = -180°$, increases as $l$ increases; e.g., it is seen from Fig. 5(a) that at $l = 0$, $f_{res} = 7.8$ GHz, and at $l = 1.5$ $mm$, $f_{res} = 10.4$ GHz. This circuit technique has been used for fine tuning of IMPATT amplifiers and oscillators [16].

c) The effect of embedding on the phase variation varies with frequency; at frequencies above the crossover frequency $f_0$, embedding improves the phase variation while at lower frequencies it is reduced. The crossover frequency $f_0$ is determined primarily by the series resonant frequency of the bond-wire inductance $L_W$ and the mean varactor capacitance $C_{jm}$

$$C_{jm} = | C_j(0) + C_j(V_{br}) |/2. \quad (1)$$

To obtain a large reflection phase variation, the magnitude of the reactance of the junction capacitance must be such that

$$\left| \frac{1}{\omega C_{jm}} \right| \gtrsim \omega L_W. \quad (2)$$

TABLE III
PHASE CHARACTERISTICS OF FOUR VARACTOR-DIODE TYPES

| | PHASE-FREQUENCY SLOPE (DEGREES/GHz) | | |
|---|---|---|---|
| $l$ (mm) | 0 | 0.75 | 1.5 |
| DIODE TYPE | | | |
| BXY53 | -18.5 | -16 | -11.5 |
| ML4704 | -19 | -15 | -9 |
| ML4707 | -14.5 | -13.5 | -10 |
| GC1600-30 | -18.5 | -16 | -15 |

| | PHASE VARIATION AT 10 GHz (DEGREES) | | |
|---|---|---|---|
| $l$ (mm) | 0 | 0.75 | 1.5 |
| DIODE TYPE | | | |
| BXY53 | 62 | 82 | 127 |
| ML4704 | 78 | 92 | 115 |
| ML4707 | 42 | 48 | 74 |
| GC1600-30 | 94 | 76 | 54 |

Thus, if a low-capacitance varactor is used to realize a large reactance change and a consequent large reflection phase change, then a large bond-wire inductance is required to reduce the crossover frequency to below the operating frequency for an improved change upon embedding.

The crossover frequencies for the devices in order of decreasing varactor capacitance shown in Fig. 4 were measured approximately as 6.8, 7.4, 8.6, and 12.2 GHz. The four devices have reflection phase characteristics at 10 GHz as summarized in Table III. The BXY53 and ML4704 devices exhibit similar behavior while the ML4707 exhibits an inferior phase variation. All three varactors showed improved characteristics upon embedding. On the other hand, the GC1600 device exhibits a degraded reflection phase variation upon embedding and the greatest reflection phase variation for the normally mounted condition. These characteristics are further considered in Section IV in relation to wide-band tuning.

### C. Computed Varactor Phase Characteristics

The varactor reflection phase characteristics of the end-mounted embedded arrangement, $l = 1.5$ mm, are now computed to further indicate the reflection phase dependence on bond-wire inductance and varactor junction capacitance. The computed characteristics at 10 GHz are given in Fig. 6 for three bond-wire inductances of 700, 350, and 175 pH which correspond approximately to the use of nail-, $V$-, and $X$-bond arrangements. It is seen that the computed reflection phase converges at low varactor junction capacitances to the open-circuit package phase and at high varactor junction capacitances to the resonant phase of the bond-wire and package capacitance. Furthermore, the computed reflection phase variation, for

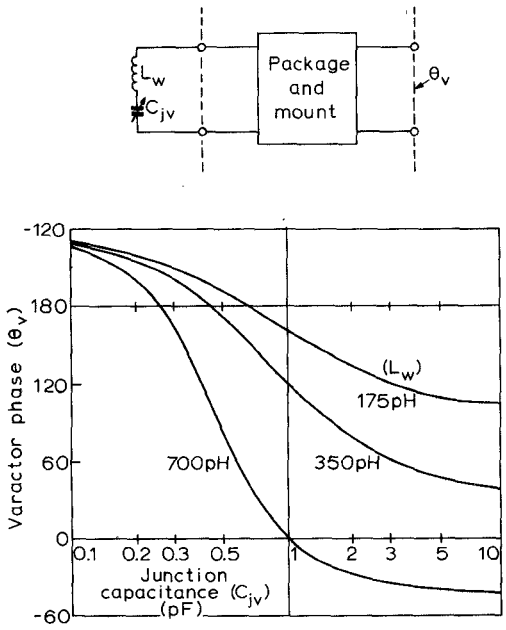


Fig. 6. Computed phase characteristics of embedded mounting at 10 GHz for different bond-wire inductances.

a given capacitance change, improves as the bond-wire inductance is increased and the mean capacitance is decreased in accordance with (2). If the BXY53 capacitance characteristics of Fig. 4 are considered in relation to the computed reflection phase characteristics of Fig. 6, then it is seen that the two wire or $V$-bond is near to optimum for a large phase variation at $X$ band. However, if the low-capacitance varactor GC1600 is considered, it is seen that the two-wire bond employed is unsatisfactory and the single-wire bond is more appropriate.

## III. THEORY OF WIDE-BAND VARACTOR-TUNED OSCILLATORS

Consider the equivalent circuit of the varactor-tuned oscillator shown in Fig. 7 where the varactor diode, active diode, cavity, and load are represented by $R_v + jX_v$, $-R_d + jX_d$, $R_c + jX_c$, and $R_L + jX_L$, respectively, in series. The elements of the equivalent circuit are effective components and have complex reactance-frequency characteristics since they include the effect of package reactances and coupling networks. The condition for oscillation requires a zero loop impedance as given by

$$Z_v + Z_{\text{eff}} = 0. \tag{3}$$

If the oscillator stability is considered with regard to the tuning voltage $V$ and frequency $f$, then

$$\frac{\delta f}{\delta V} = \frac{-\dfrac{\partial X_v}{\partial V}}{\dfrac{\partial X_v}{\partial f} + \dfrac{\partial X_{\text{eff}}}{\partial f}} \tag{4}$$

where

$$\frac{\partial X_{\text{eff}}}{\partial f} = \frac{\partial X_d}{\partial f} + \frac{\partial X_c}{\partial f} + \frac{\partial X_L}{\partial f}. \tag{5}$$

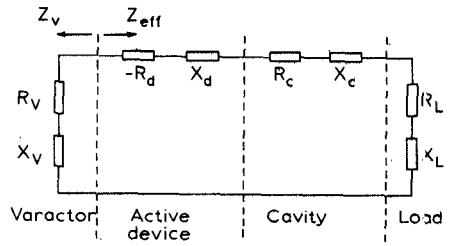


Fig. 7. Equivalent circuit of series varactor-tuned oscillator.

From (4) it is seen that the tuning range is improved if the voltage dependence of the effective varactor reactance is increased or if the frequency dependence of the effective circuit reactance $X_{\text{eff}}$ is reduced.

If the coupling to the varactor is increased, then the effective voltage dependence of the varactor reactance is also increased. If in the equivalent circuit of Fig. 7 the circuit elements are normalized to a circuit impedance $Z_0$, then the coupling to the varactor is increased if the varactor diode is coupled to the circuit via a lower impedance $Z_c$ transmission line. If $X_v'$ is the reactance of the coupled varactor, then

$$\frac{\partial X_v'}{\partial V} = \left(\frac{Z_0}{Z_c}\right)\frac{\partial X_v}{\partial V}. \tag{6}$$

This improvement is obtained at the expense of increased power absorbed in the varactor loss resistance $R_v$. For a given varactor, it is possible to write

$$\frac{\partial X_v}{\partial V} = A\,\frac{\partial X_v}{\partial f} \tag{7}$$

where $A$ is a function of the coupling between the varactor and the circuit.

Substituting (7) into (4) we obtain

$$\frac{\delta f}{\delta V} = A\,\frac{-\dfrac{\partial X_v}{\partial f}}{\dfrac{\partial X_v}{\partial f} + \dfrac{\partial X_{\text{eff}}}{\partial f}}. \tag{8}$$

For a given variation circuit-device-load reactance with frequency $\partial X_{\text{eff}}/\partial f$, a large tuning range is obtained by increasing $\partial X_v/\partial f$. This is also implied in (2), given previously, and can be achieved by using small capacitance varactors [3] in miniature packages [1] or by using two or more larger capacitance varactors connected in series [2]. An inspection of (8) further indicates that very large tuning ranges are possible if either the effective circuit reactance $X_{\text{eff}}$, or the varactor reactance $X_v$ frequency slopes are reduced, or if the slopes are made nearly equal and opposite. This latter situation is known as reactance compensation and is commonly used for broad-banding the gain/frequency response of parametric amplifiers [17]. The technique when applied to wide-band varactor-tuned oscillators was first suggested [18] and experimentally reported by Aitchison [19]. The improved tuning ranges are obtained at the expense of a decreased oscillator $Q$.

Since oscillator $Q$ determines noise and stability, too low a value may be undesirable. Large tuning ranges involve high RF varactor voltage swings as a result of tight coupling and the mean varactor capacitance increases. This effect is particularly noticeable at low tuning voltages [8] and can lead to a substantial self-bias voltage which reduces the tuning range [7].

## IV. ELECTRONICALLY TUNABLE OSCILLATORS

### *A. Tuning Range Prediction from Varactor Reflection Phase Characteristics*

The varactor reflection phase characteristics are now considered in relation to wide-band varactor tuning ranges. The effect of varactor reflection phase on oscillator tuning range is illustrated in Fig. 8. The lowest frequency of oscillation, $f_1$, occurs at zero varactor bias and the highest frequency, $f_2$, at breakdown. The "tuning phase," $\gamma$, is given by the degree of overlap of the two phase curves $\theta(f_1)$ and $\theta(f_2)$. The varactor phase at the lowest frequency, $\theta_0(f_1)$, is given by

$$\theta_0(f_1) = \theta_{br}(f_1) - \Delta\theta(f_1). \tag{9}$$

Similarly, the varactor phase at the highest frequency, $\theta_{br}(f_2)$, is given by

$$\theta_{br}(f_2) = \theta_0(f_2) - \Delta\theta(f_2). \tag{10}$$

If it is required to maximize the tuning range $\Delta f$

$$\Delta f = f_2 - f_1 \tag{11}$$

then it is required that the tuning phase, $\gamma$, be a maximum

$$\gamma = \theta_{br}(f_2) - \theta_0(f_1). \tag{12}$$

Combining (9) and (12)

$$\gamma = \Delta\theta(f_1) - [\theta_{br}(f_1) - \theta_{br}(f_2)] \tag{13}$$

and similarly combining (10) and (12)

$$\gamma = \Delta\theta(f_2) - [\theta_0(f_1) - \theta_0(f_2)]. \tag{14}$$

From (13) and (14), to maximize $\gamma$, it is required to a) maximize the varactor reflection phase variation over the tuning range; and b) minimize or possibly change the frequency slope of the varactor reflection phase. These two effects are also implied by (4). They are equivalent to increasing the coupling to the varactor diode and decreasing the oscillator $Q$ by reactance compensation.

Equations (13) and (14) are now used to predict the varactor tuning properties of the four devices given in Table III. It is seen that the tuning phase of the BXY53 and ML4704 are very similar, and hence similar tuning ranges at $X$ band in a varactor-tuned oscillator are predicted. The ML4707 exhibits an inferior tuning phase even though the slope of breakdown phase-frequency is less than that of the two previous devices. The GC-1600 device shows the greatest tuning phase for the normally mounted arrangement, but this device exhibits a degraded tuning phase upon embedding when compared with the other devices. The results indicate that improved tuning phases are dependent upon the varactor junction capacitance, the bond-wire configuration, and the stray parasitic reactances of the package and circuit. These considerations have been employed in the design of wide-band varactor-tuned oscillators as discussed in the following sections.

### *B. Performance of Three Coaxial Oscillators*

The three coaxial cavity configurations shown schematically in Fig. 9 have been investigated. Bias feeds and decoupling networks have been neglected for simplicity. The first two show series arrangements and the third a parallel arrangement of varactor and active devices. In the first arrangement the active device is end-mounted and in the second and third arrangements it is shunt-mounted. All three oscillators use a nominal quarter-wavelength low-impedance-matching section. In the series arrangements, the separation of the varactor and active

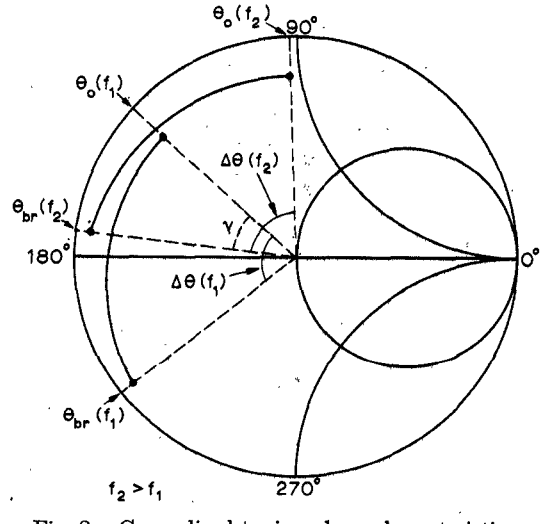


Fig. 8. Generalized tuning phase characteristics.

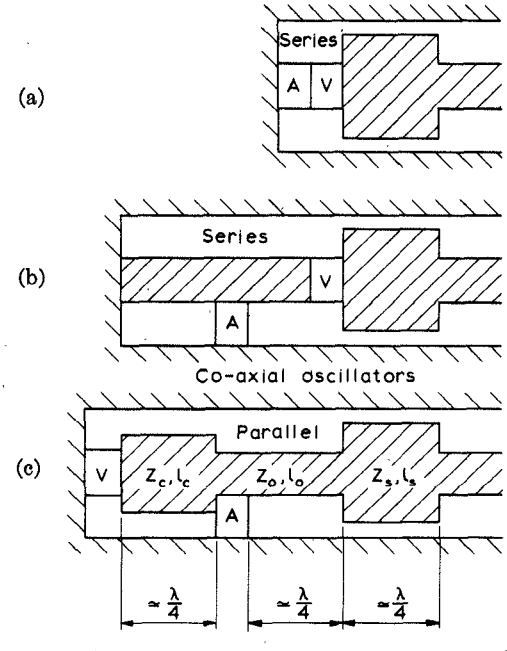


Fig. 9. Schematics of three coaxial varactor-tuned oscillators.

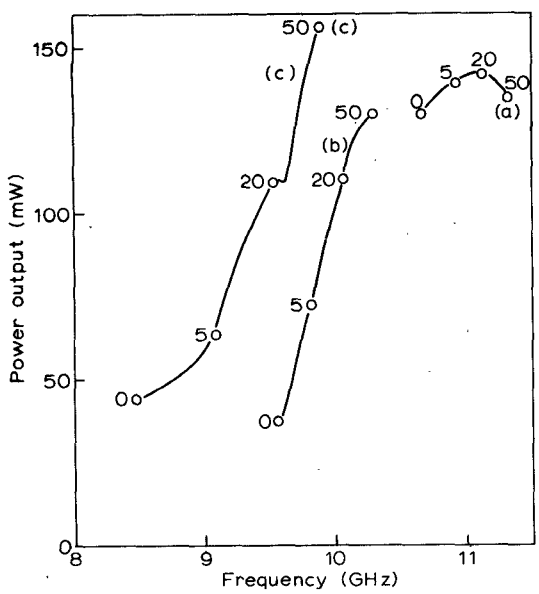


Fig. 10. Performance of three coaxial varactor-tuned oscillators.

devices is controlled by the geometry of the S4 package. The parallel arrangement, however, does not suffer from this limitation as a nominal quarter-wavelength line is placed between the devices. The second series arrangement essentially differs from the one reported by Grace [20] in that the active and varactor diodes are interchanged and the active diode is connected to ground for improved heat sinking. The tuning ranges of the series arrangements were less than the tuning range of the parallel arrangement as shown in Fig. 10. It is seen that the approximate tuning bandwidth of the series arrangements are 6.5 and 7.5 percent and the parallel arrangement is 15 percent. The performance is given for a Mullard CXY 19 Gunn device, similar to that used by Joshi [7], and a Mullard BXY53 tuning varactor. The Gunn-diode dc voltage is approximately 12 V at a current of approximately 500 mA. The varactor diode was mounted normally, $l = 0$ mm, in all three oscillator arrangements.

### C. Wide-Band Operation

Wide-band varactor-tuned performance was accomplished from the use of the embedded varactor-diode arrangement and a choice of varactor parameters, including bond-wire inductance, from improved tuning phase considerations that were discussed previously. For the series arrangements, the embedded arrangement was achieved by recessing the varactor-diode package in the low-impedance output-matching section.

The tuning performance of the parallel oscillator is shown in Fig. 11 using a BXY53 varactor and CXY19 Gunn device. The tuning ranges increase from approximately 1.4 GHz at $l = 0$ mm, through 1.7 GHz at $l = 0.75$ mm, to 2.4 GHz at $l = 1.5$ mm. The overall improvement in tuning range is greater than 70 percent. Substantial improvements in the tuning range of the series oscillators were also observed. The improvements for the oscillators shown schematically in Fig. 9(a) and (b) were more than 150 and 110 percent, respectively. The improved tuning ranges are the result of reactance compensation as discussed in Section III, and were accompanied by a decrease in output power due to the increased coupling to the varactor loss.

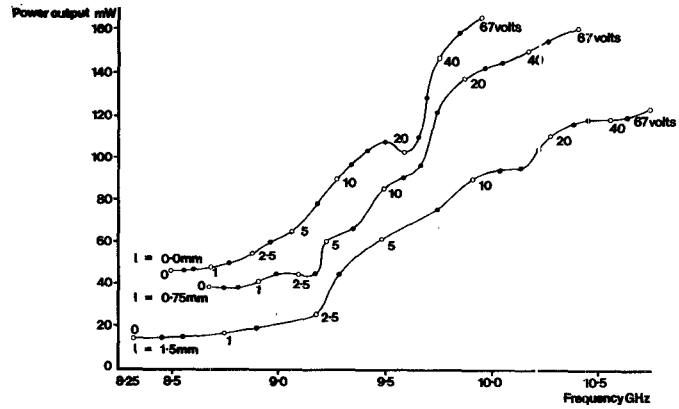


Fig. 11. Wide-band tuning performance of parallel oscillator.

The tradeoff in oscillator output power and tuning range can be found only from analysis of the particular oscillator equivalent circuit. An analysis of the parallel oscillator using an IMPATT diode has shown [9] that substantial agreement with measured tuning range was evident and the greater output variation and reduced tuning ranges of the IMPATT diode were a consequence of the higher device $Q$. Similar observations have been reported by Johnson [2].

The effect of changing the coupling circuit impedance for different varactor-mounting arrangements is given in Table IV. The ML4704 varactor was used and the cavity dimensions were $l_c = 6$ mm, $l_0 = 5$ mm, and $l_m = 7.5$ mm. It is seen that at a particular varactor mounting the frac-

TABLE IV
VARACTOR-TUNED OSCILLATOR PERFORMANCE FOR DIFFERENT CIRCUIT IMPEDANCES AND VARACTOR-DIODE MOUNTING CONDITIONS

| $Z_C$ (Ω) | | ℓ (mm) 0 | 0.75 | 1.5 |
|---|---|---|---|---|
| | fmin GHz | 7.39 | 7.46 | 7.21 |
| 20 | Δf GHz | 2.09 | 2.46 | 2.97 |
| | Bf % | 24.8 | 28.3 | 34.2 |
| | fmin | 8.30 | 8.39 | 7.99 |
| 30 | Δf | 1.93 | 2.31 | 3.03 |
| | Bf | 20.8 | 24.2 | 31.9 |
| | fmin | 8.80 | 8.95 | 8.40 |
| 40 | Δf | 1.90 | 2.06 | 2.92 |
| | Bf | 19.5 | 20.7 | 29.7 |
| | fmin | 9.41 | 9.49 | 8.72 |
| 50 | Δf | 1.70 | 1.88 | 2.83 |
| | Bf | 16.6 | 18.0 | 27.9 |

tional tuning bandwidth, $B_f$, i.e., the tuning range $\Delta f$ normalized with respect to the midband frequency, increases as the coupling circuit impedance $Z_c$ is reduced in accordance with (6). The maximum tuning range of 3.03 GHz (31.9 percent) at $Z_c = 30\ \Omega$ and bandwidth 34.2 percent (2.97 GHz) at $Z_c = 20\ \Omega$ are, to the authors' knowledge, the largest reported with devices in S4 packages in a distributed circuit and exceed previous reports [6]–[8], [19], [20].

### D. Parallel Oscillator Construction

A sectional drawing of the oscillator is given in Fig. 12. An integral bias unit is used to apply a common floating dc bias to the active device and varactor diode. The RF leakage is more than 30 dB down and the insertion loss of the unit is less than 0.2 dB. Finally, an inner break decouples the common-bias inner line from the load and a thin sheet of Melinex decouples the outer line varactor voltage from the active-diode bias voltage. A photograph of the oscillator is given in Fig. 13.

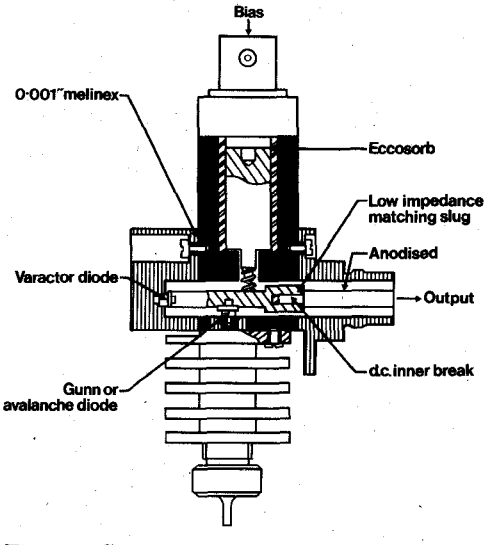


Fig. 12. Sectional drawing of parallel oscillator.

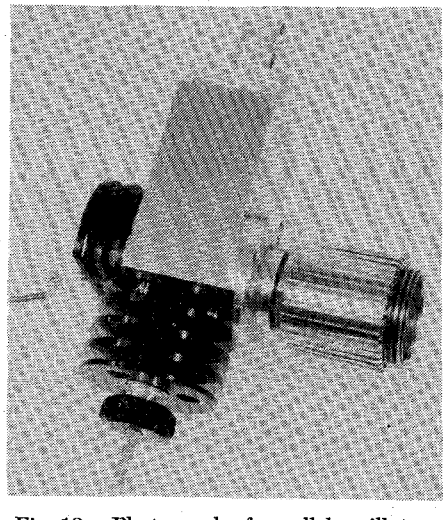

Fig. 13. Photograph of parallel oscillator.

## V. CONCLUSIONS

It has been shown experimentally that package and circuit stray reactances affect the tuning range of varactor-tuned oscillators. In particular, a simple circuit technique was employed to modify the mount parasitics of a coaxially end-mounted S4 package. Package and circuit stray reactances, varactor capacitance, and bond-wire inductance were shown to noticeably affect the varactor-diode tuning characteristics. Equivalent-circuit models were developed which showed very good agreement with the measured impedance. A general theory of varactor-tuned oscillators was developed and the impedance characteristics of the varactor and circuit were related to tuning range. These results were used to design three coaxial varactor-tuned oscillators and a tuning range in excess of 3 GHz at $X$ band was reported for the parallel arrangement. Furthermore, Gunn devices were shown to be superior to IMPATT diodes for wide-band tuning. In general, improved tuning ranges were shown to be due to an increased coupling to the varactor diode and to a decreased oscillator $Q$ by reactance compensation.

## ACKNOWLEDGMENT

The authors wish to thank C. S. Aitchison and B. H. Newton for their many helpful ideas and discussions on varactor-tuned oscillators and diode characterization, and F. C. de Ronde for the design of the coaxial bias unit.

## REFERENCES

[1] D. Large, "Octave band varactor tuned Gunn diode sources," *Microwave J.*, vol. 13, p. 49, Oct. 1970.
[2] K. M. Johnson, "Wide bandwidth IMPATT and Gunn voltage-tuned oscillator," in *IEEE G-MTT Int. Microwave Symp. Dig.* (Chicago, IL), May 22–24, 1972, pp. 185–186.
[3] R. A. Gough and B. H. Newton, "An integrated wide-band varactor-tuned Gunn oscillator," *IEEE Trans. Electron Devices*, vol. ED-20, pp. 863–865, Oct. 1973.
[4] R. P. Owens, "Mount-independent equivalent circuit of the S4 package," *Electron. Lett.*, vol. 7, pp. 580–582, Sept. 1971.
[5] C. L. Upadhyayula and B. S. Perlman, "Design and performance of transferred electron amplifiers using distributed equalizer networks," *IEEE J. Solid-State Circuits* (*Special Issue on Microwave Integrated Circuits*), vol. SC-8, pp. 29–36, Feb. 1973.
[6] R. B. Smith and P. W. Crane, "Varactor tuned Gunn effect oscillators," *Electron. Lett.*, vol. 6, pp. 139–140, Mar. 1970.
[7] J. S. Joshi, "Wide-band varactor-tuned $X$-band Gunn oscillators in full-height waveguide cavity," *IEEE Trans. Microwave Theory Tech.* (Short Papers), vol. MTT-21, pp. 137–139, Mar. 1973.
[8] B. J. Downing and F. A. Myers, "Broadband (1.95 GHz) varactor-tuning $X$-band Gunn oscillator," *Electron. Lett.*, vol. 7, pp. 407–409, July 1971.
[9] C. D. Corbey, "The characteristics of IMPATT diodes in relation to wide-band varactor tuned oscillators," *Acta Electron.*, vol. 17, pp. 187–192, Apr. 1974.
[10] C. D. Corbey and R. A. Gough, "The effects of package and mount parameters on wide-band varactor tuned oscillators," in *Proc. 4th Biennial Cornell Conf. Microwave Semiconductor Devices, Circuits and Applications* (Cornell Univ., Ithaca, NY, Aug. 1973), pp. 165–175.
[11] R. A. Gough, "Varactor-tuned Gunn-effect oscillators," Ph.D. dissertation, Univ. Bradford, Bradford, Yorks., England, 1973.
[12] B. J. Downing and P. N. Robson, "Microwave-package measurement at $Q$-band," *Electron. Lett.*, vol. 9, pp. 245–246, May 1973.
[13] P. J. DeWaard, "Measurement of admittance of Gunn diodes in passive and active regions of bias voltage," *Electron. Lett.*, vol. 9, pp. 59–60, Feb. 1973.
[14] D. A. E. Roberts and K. Wilson, "Evaluation of high quality varactor diodes," *Radio Electron. Eng.*, vol. 31, pp. 277–285, May 1966.

[15] "Microwave Solid State Products," *Mullard Technical Handbook*, Mullard House, Torrington Place, London, WC1, England.
[16] Hewlett-Packard Application Note no. 935.
[17] C. S. Aitchison, R. Davies, and P. J. Gibson, "A simple diode parametric amplifier design for use at S, C, and X band," *IEEE Trans. Microwave Theory Tech.*, vol. MTT-15, pp. 22–31, Jan. 1967.
[18] C. S. Aitchison, "Method of improving tuning range obtained from a varactor-tuned Gunn oscillator," *Electron. Lett.*, vol. 10, pp. 94–95, Apr. 1974.
[19] ——, "Gunn oscillator electronic tuning range and reactance compensation: An experimental result at X-band," *Electron. Lett.*, vol. 10, pp. 488–489, Nov. 1974.
[20] M. I. Grace, "Varactor-tuned avalanche transit-time oscillator with linear tuning characteristics," *IEEE Trans. Microwave Theory Tech.* (Corresp.), vol. MTT-18, pp. 44–45, Jan. 1970.

# On the Design of Dielectric Loaded Waveguides

TALAL K. FINDAKLY, STUDENT MEMBER, IEEE, AND HAIM M. HASKAL, SENIOR MEMBER, IEEE

*Abstract*—**Rectangular waveguides partially filled with a dielectric slab in the $E$ plane can provide an alternative to ridged waveguides in broad-band systems. It is shown that by an appropriate choice of the dielectric constant, maximum power handling capacity for a given bandwidth and cutoff wavelength can be achieved. This power handling capacity is much higher than for ridged waveguides. Attenuation and the effect of the first longitudinal-section-electric (LSE) mode on bandwidth are also discussed.**

## INTRODUCTION

DIELECTRIC loaded waveguides have been investigated by a number of authors [1]–[6] in the past two decades. In particular, a rectangular waveguide loaded with a dielectric slab across its center, in the $E$ plane, manifests attractive properties as a transmission medium: increased bandwidth, greatly increased power handling capacity, and relatively low attenuation.

For broad-band systems, ridged waveguides are currently in use. Their properties were analyzed in detail by Hopfer [7]; standard lines of ridged waveguides designed for fixed bandwidths and minimum attenuation are available. The potential advantage of dielectric loaded waveguides over ridged waveguides is in the power handling capacity. The purpose of this paper is to present a design procedure which maximizes the power handling capacity of dielectric loaded rectangular waveguides. It will be shown that for a given cutoff frequency, the maximum power handling capacity is obtained when a dielectric slab is chosen having the smallest dielectric constant consistent with the bandwidth requirements. This dielectric constant then determines uniquely the dimensions of the slab and of the waveguide. The resultant waveguide has a bandwidth, dimensions, and attenuation comparable to those of the ridged waveguide but a power handling capacity about six to seven times higher around the frequency of minimum attenuation.

Previous work analyzed the propagation characteristics of the $TE_{n,0}$, longitudinal-section-electric (LSE), and longitudinal-section-magnetic (LSM) modes in the dielectric loaded waveguide. The present paper discusses in detail the characteristics of the first LSE mode and its effect on bandwidth.

## THEORY

The geometry of the dielectric loaded guide under consideration is shown in Fig. 1. The modes which can propagate in this inhomogeneously filled waveguide are of two types [8]: LSE modes characterized by $E_x = 0$ and LSM modes with $H_x = 0$. LSE modes with no $y$ dependence reduce to the ordinary $TE_{n,0}$ modes. The bandwidth of the loaded waveguide is normally defined as the ratio of cutoff frequencies of the $TE_{20}$ to the $TE_{10}$ modes. This has been discussed previously [3]; for convenience, we reproduce here (Fig. 2) bandwidth curves similar to those in that paper. The important conclusion to draw from these curves is that for a given bandwidth, a relative dielectric constant $K'$ greater than a critical value must

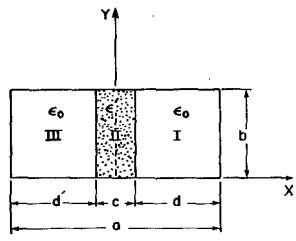


Fig. 1. Waveguide cross section.

Manuscript received January 27, 1975; revised June 2, 1975.
T. K. Findakly was with the Department of Electrical Engineering, Tufts University, Medford, MA. He is now with the Department of Electrical Engineering, Purdue University, Lafayette, IN 47906.
H. M. Haskal is with the Department of Electrical Engineering, Tufts University, Medford, MA 02155.